

Preparation and characterization of $\text{LiNi}_{0.8}\text{Co}_{0.2}\text{O}_2$ synthesized by an emulsion drying method

TAE-HYUNG CHO and HOON-TAEK CHUNG*

Department of Ceramic Engineering, Dongshin University, 252 Daeho-dong, Naju, Chonnam, 520-714, South Korea
(*author for correspondence, fax: +82-61-330-2909; e-mail: htchung@dsu.ac.kr)

Received 9 June 2002; accepted in revised form 3 May 2005

Key words: cathode, emulsion drying method, $\text{LiNi}_{0.8}\text{Co}_{0.2}\text{O}_2$, Rietveld analysis, secondary lithium battery

Abstract

A layered $\text{LiNi}_{0.8}\text{Co}_{0.2}\text{O}_2$ solid solution, which is a promising cathode material for secondary lithium batteries, was successfully synthesized by an emulsion drying method. Because electrochemical properties significantly depend on the conditions of the synthesis, the calcination temperature was carefully determined on the basis of X-ray diffraction and TG studies. The prepared cathodes were characterized by means of SEM, BET, X-ray diffraction, Rietveld refinement, cyclic voltammetry and a charge-discharge experiment. From the Rietveld analysis, it was found that powder calcined at 800 °C for 12 h exhibits a well ordered and lower cation mixed layered structure than the others. The cyclic voltammetry experiment shows that phase transformation can be suppressed considerably by increasing the calcination temperature to 800 °C. The highest discharge capacity of 188.4 mA h g⁻¹ was obtained from the sample prepared at 800 °C. Furthermore, a high capacity retention ratio of 88.1% was found for the initial value after 50 cycles at a constant current density of 40 mA g⁻¹ between 2.7 V_{Li/Li}⁺ and 4.3 V_{Li/Li}⁺. In the rate capability test, the cathode delivered a higher discharge capacity of 153.1 mA h g⁻¹ at a 4 C (800 mA g⁻¹) rate.

1. Introduction

The layered transition metal oxide LiNiO_2 is a promising cathode material for secondary lithium batteries because of its high reversible capacity and because it has a lower cost and lower toxicity than commercially used LiCoO_2 . However, it has some disadvantages such as nonstoichiometry (called cation mixing), degradation of the retention capacity due to a structural change during the cycling [1], and thermal instability at a highly oxidized state. Partial substitution of other elements (Co, Mn, Fe, Al, Zr, and Ti) for Ni sites has been studied to improve the electrochemical performance of LiNiO_2 [2–8]. Of these elements, cobalt has attracted much attention because only cobalt substitution can form a complete solid solution, and the solid solution shows better thermal stability than pristine LiNiO_2 . Moreover, according to Rougier et al. and Saadoun et al., quasi-2D structure compounds can be obtained by substituting more than 20% of the Ni with Co [9–10]. Thus, $\text{LiCo}_x\text{Ni}_{1-x}\text{O}_2$ ($x = 0.2$ – 0.3) is an efficient system for stabilizing the thermal and electrochemical properties of LiNiO_2 [10–12].

The electrochemical properties of LiNiO_2 and $\text{LiNi}_{1-x}\text{Co}_x\text{O}_2$ are strongly affected by the synthesis conditions. To obtain a homogeneous mixture, a conventional solid-state reaction method generally requires a long

calcination time, as well as precalcination and intermittent grinding. Soft chemistry, on the other hand, which enables a solid phase to be formed through a chemical reaction in a liquid phase at a moderate temperature, has some advantages in obtaining a homogeneous solid solution and powder with small particles. As a result, the cathode materials prepared with soft chemistry show smaller a I-R drop and higher chemical diffusivity [13], shorter calcination times [12] and small particles that can enhance the reversible capacity [14].

In our previous work, we successfully introduced a simple synthetic method, namely the emulsion drying method, to prepare homogeneously substituted cathode materials [15, 16]. Using this method, we readily obtained homogeneous material with small particles. In this study, therefore, we applied the emulsion drying method as a synthetic route for preparing layered $\text{LiNi}_{0.8}\text{Co}_{0.2}\text{O}_2$, and investigated the dependence of structural and electrochemical properties on the synthesis conditions.

2. Experimental

For the starting materials, we used LiNO_3 , $\text{Ni}(\text{NO}_3)_2 \cdot 6\text{H}_2\text{O}$ and $\text{Co}(\text{NO}_3)_2 \cdot 6\text{H}_2\text{O}$. The $\text{LiNi}_{0.8}\text{Co}_{0.2}\text{O}_2$ powders were synthesized with the emulsion drying method,

the detail of which has been reported elsewhere [17]. The synthesized powders were calcined under an oxygen flow with a heating rate of $5\text{ }^{\circ}\text{C min}^{-1}$ in the temperature range $700\text{--}850\text{ }^{\circ}\text{C}$ for 12 h.

We obtained the XRD patterns of the calcined powders for structural analysis by using an X-ray powder diffractometer (CuK α radiation) and we collected the data in steps of 0.03 (2θ) in the range $10\text{--}100$ (2θ) with a constant counting time of 10 s per step. Rietveld refinements were performed with the aid of the *FullProf* 2000 program [18]. Scanning electron microscopy (SEM) was used to observe how the powder morphology varied in relation to the calcination temperatures. To measure specific surface areas of the synthesized materials, we used the BET method with the aid of a Micromeritics Gemini 2375 (USA).

Electrochemical studies were conducted on Li/LiPF₆ in EC-DMC (1:2 in Vol.)/LiNi_{0.8}Co_{0.2}O₂ cells. We prepared the positive electrodes by blending the active materials with acetylene black and PVdF in a weight ratio of 90:6:4 in NMP. We then spread the slurry on 1 cm^2 nickel ex-met and dried it in a vacuum oven at $120\text{ }^{\circ}\text{C}$ for 2 days. The cell was assembled in a glove box filled with high purity Ar gas. Using a WBCS3000 (Wonatech, Korea) battery cycle tester, we applied a constant current of 40 mA g^{-1} to the working electrode for the charge-discharge experiment that was conducted in the voltage range of $4.3\text{ V}_{\text{Li/Li}}^+$ to $2.7\text{ V}_{\text{Li/Li}}^+$ and we applied a constant current of 200 mA g^{-1} for the experiment conducted in the range of $4.2\text{ V}_{\text{Li/Li}}^+$ to $2.7\text{ V}_{\text{Li/Li}}^+$. We conducted cyclic voltammetry experiments at a scan speed of 0.1 mV s^{-1} between 2.7 and 4.3 V versus Li/Li⁺.

3. Results and discussion

Figure 1 shows a thermogravimetric curve for the dried emulsion precursor of LiNi_{0.8}Co_{0.2}O₂. The thermogravimetric profile had time steps of weight loss. The first

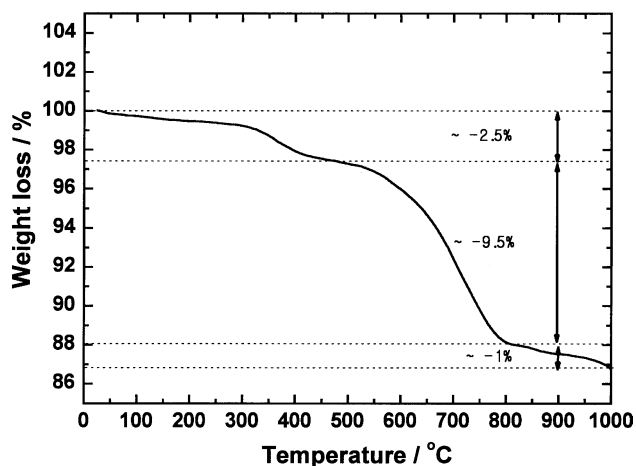


Fig. 1. TGA curve for the LiNi_{0.8}Co_{0.2}O₂ precursor obtained by the emulsion drying method.

step, which was observed around $370\text{ }^{\circ}\text{C}$, had a 2.5% weight loss. We attributed this loss mainly to the combustion of residual organic compounds such as the kerosene and the surfactant that remains after the burnout process [17]. The second step, which started at $500\text{ }^{\circ}\text{C}$ and finished around $800\text{ }^{\circ}\text{C}$, had a 9.5% weight loss. To elucidate the origin of the second weight loss, we applied an XRD experiment for the samples calcined at $500\text{ }^{\circ}\text{C}$ and $700\text{ }^{\circ}\text{C}$. We chose these temperatures because they represent the starting point and middle point of the second weight loss.

Figure 2 shows the results of the X-ray diffraction experiment. As can be seen in Figure 2(a), the powder calcined at $500\text{ }^{\circ}\text{C}$ shows the mixed phases of a hexagonal lattice with Li₂CO₃ and NiO. However, when we increased the calcination temperature to $700\text{ }^{\circ}\text{C}$ (see Figure 2(b)), the NiO phase was eliminated and we observed only a small amount of the Li₂CO₃ and well-developed LiNi_{0.8}Co_{0.2}O₂ hexagonal phases. These results indicate that the second weight loss in the thermogravimetric profile is related to the evaporation of the CO_x gas produced by the reaction of Li₂CO₃ and NiO. The third weight loss, observed at around $825\text{ }^{\circ}\text{C}$, may be due to the evaporation of lithium and oxygen [19]. On the basis of these results, we therefore determined the appropriate calcination temperature to be between $750\text{ }^{\circ}\text{C}$ and $850\text{ }^{\circ}\text{C}$.

Figure 3 shows typical XRD patterns of the synthesized LiNi_{0.8}Co_{0.2}O₂ materials at calcination temperatures of 750 , 800 and $850\text{ }^{\circ}\text{C}$. We refer to the materials synthesized at these temperatures as E75, E80 and E85, respectively. The XRD patterns of all materials were indexed based on the a-NaFeO₂ structure (space group: 166, R3 m) and we observed no secondary phase in the entire scan range. The lattice parameters of the synthesized LiNi_{0.8}Co_{0.2}O₂ materials were calculated by Rietveld refinement, the results of which are summarized in Table 1 along with a summary of specific surface areas. As shown in Table 1, the lattice parameters a and c

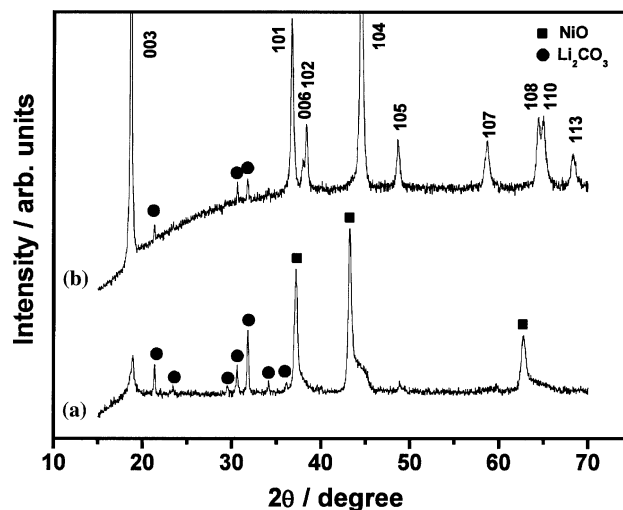


Fig. 2. XRD patterns of LiNi_{0.8}Co_{0.2}O₂ powders calcined at (a) $500\text{ }^{\circ}\text{C}$ and (b) $700\text{ }^{\circ}\text{C}$ for 12 h under an oxygen flow.

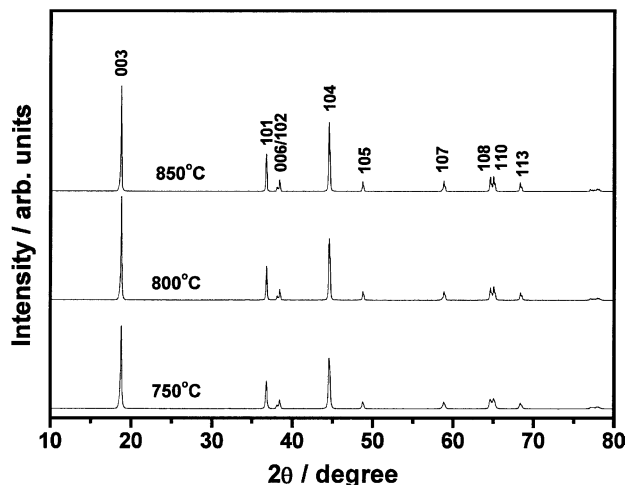


Fig. 3. XRD patterns of $\text{LiNi}_{0.8}\text{Co}_{0.2}\text{O}_2$ powders synthesized at different temperatures.

increase slightly as the calcination temperature increases, whereas the c/a values, which indicate the disorder of the hexagonal structure [20], are almost unchanged.

The values of the cation mixing obtained with the aid of Rietveld refinement differ slightly. The cation mixing values obtained with XRD profile refinement were 1.1% for E75, 0.5% for E80, and 1.9% for E85. Our samples show a negligible amount of cation mixing, especially the E80, which has a value very close to the ideal structure. In this compound, cation mixing is important because the Ni-based layered cathode material suffers from cation mixing. When cation mixing occurs in the layered structure, some nickel ions are divalent and lead to the $[\text{Li}_{1-x}\text{Ni}_x^{2+}][(\text{Ni}_{1-x}^{3+}\text{Ni}_x^{2+})_{0.8}\text{Co}_{0.2}]\text{O}_2$ formula [9]. The divalent nickel ion in the lithium site is oxidized to trivalent during the initial charging process and cannot be readily reduced. As a result, irreversible oxidation of nickel ion in the lithium site leads to shrinkage of the local interslab thickness with respect to differences in the ionic radius of Ni^{3+} (0.57 Å) and Ni^{2+} (0.70 Å). This local shrinkage of the interslab thickness hinders the lithium reintercalation into the cathode material, thereby deteriorating the electrochemical performance of factors such as cycle stability and efficiency. Therefore, E80, which has less cation mixing than E75 or E85, is expected to show a good electrochemical performance in terms of factors such as high reversible capacity and cycle stability.

Figure 4 shows the microstructures of E75, E80 and E85. Sample E75 consists of particles smaller than

0.5 μm , when we increased the calcination temperature, the particle size gradually increased and, at 850 °C, the particles increased to approximately 1 μm . This increase in particle size decreased specific surface areas. The specific surface areas were 2.37 $\text{m}^2 \text{g}^{-1}$ for E75, 1.09 $\text{m}^2 \text{g}^{-1}$ for E80 and 0.58 $\text{m}^2 \text{g}^{-1}$ for E85.

We performed electrochemical charge-discharge experiments on the synthesized $\text{LiNi}_{0.8}\text{Co}_{0.2}\text{O}_2$ materials at room temperature in the voltage range 2.7 $\text{V}_{\text{Li}/\text{Li}}$ to 4.3 $\text{V}_{\text{Li}/\text{Li}}$ with a current density of 40 mA g^{-1} . Figure 5 shows the initial charge-discharge curves and the cycling performance as a function of the number of cycles.

Figure 5(a) shows high initial discharge capacities of 183 mA h g^{-1} for E75, 188.44 mA h g^{-1} for E80 and 182.23 mA h g^{-1} for E85. Furthermore, the irreversible capacity losses were 9.6% for E75, 7.3 percent for E80, and 11.7% for E85. E80 shows the highest initial discharge capacity as well as the lowest irreversible capacity loss in the initial charge-discharge process.

Figure 5(b) shows the cycle stability of each sample over 50 cycles. Although the difference in capacity retention among the samples was not large, E80 had the highest capacity retention ratio of 88.1% for the initial capacity and E75 had the lowest capacity retention ratio of 86.8%. The difference became clear when the cathode material was cycled at a 1 C rate (200 mA g^{-1}) in the voltage range 2.7 $\text{V}_{\text{Li}/\text{Li}}$ to 4.2 $\text{V}_{\text{Li}/\text{Li}}$.

Figure 6 shows the results of the 1 C rate cycling test. Over 100 cycles, the E80 sample has better cycle stability than the other samples. After 100 cycles, the capacity retentions were 78.8% for E75, 86.1% for E80 and 81.3 percent for E85.

With respect to the phase transformation during the charge-discharge process, the cycle life is related to the cathode material structural damage is induced by stress or fractures in the particles or both [1, 21, 22]. To observe the phase transformation, we used cyclic voltammetry because such experiments are useful for observing phase transformation during the lithium intercalation and deintercalation processes [21].

Figure 7 shows a typical cyclic voltammogram of the first five cycles of $\text{LiNi}_{0.8}\text{Co}_{0.2}\text{O}_2$. E75 shows a major oxidation peak at 3.96 $\text{V}_{\text{Li}/\text{Li}}$ and a minor oxidation peak at around 4.2 $\text{V}_{\text{Li}/\text{Li}}$ in the first oxidation process. In subsequent cycles, the major oxidation peak shifted to the lower voltage and another minor oxidation peak emerged at around 4.0 $\text{V}_{\text{Li}/\text{Li}}$. However, the minor oxidation peak diminished as the calcination temperature increased to 800 °C, and no other shoulder redox peak emerged

Table 1. Calculated structure parameters and specific surface area for the synthesized compounds

Calcination Temp./°C	Lattice parameter		c/a	Unit cell vol./Å ³	Cation mixing	Reliable factor		Specific surface area/m ² g ⁻¹
	$a/\text{Å}$	$c/\text{Å}$				R_{wp}	R_{B}	
750	2.8641(2)	14.163(1)	4.944	100.62	1.1%	13.1	1.96	2.37
800	2.8648(1)	14.164(1)	4.944	100.67	0.5%	12.5	2.04	1.09
850	2.8660(1)	14.164(1)	4.942	100.76	1.9%	13.6	3.05	0.58

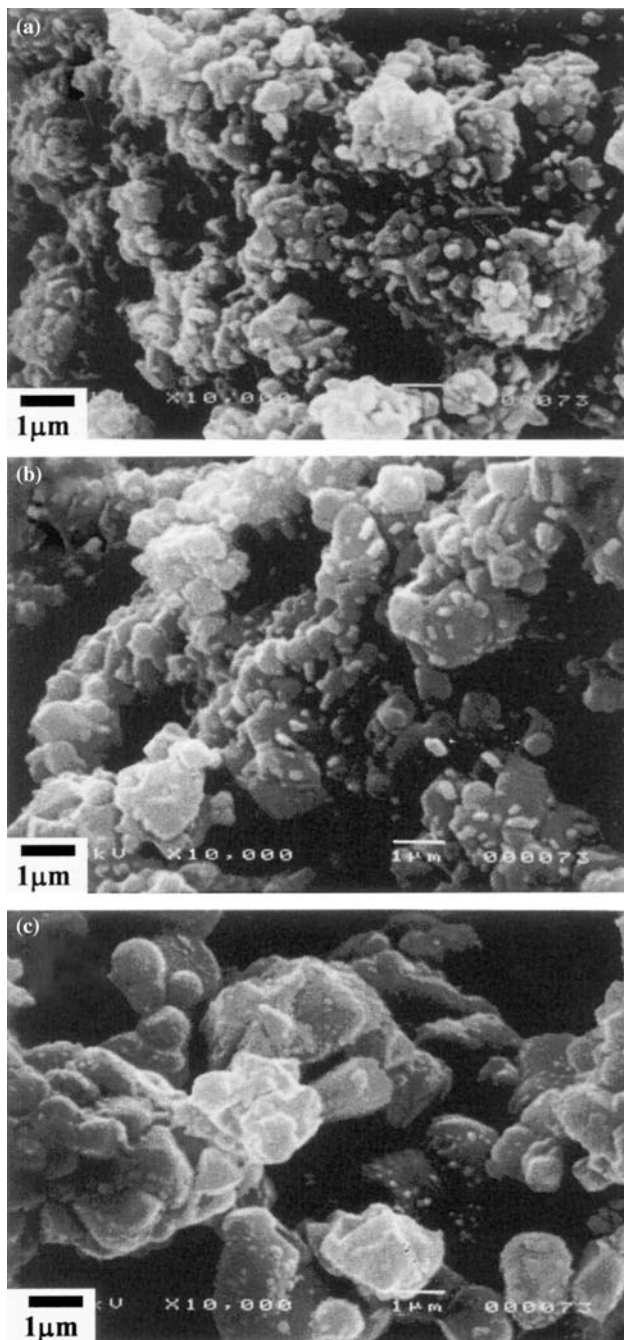


Fig. 4. SEM photographs of $\text{LiNi}_{0.8}\text{Co}_{0.2}\text{O}_2$ powders calcined at (a) 750 °C, (b) 800 °C and (c) 850 °C.

in subsequent cycles for the samples prepared at 800 °C and 850 °C. Therefore, the phase transformations are considerably suppressed as the calcination temperature increases.

To confirm the structural change after the cycling test, we used *ex situ* X-ray diffraction with a cycled electrode. Figure 8 shows the X-ray profiles. We calculated the structural parameters of the cycled cathodes by the least squares method using the ten highest diffraction lines. Table 2 compares the structural parameters of the pristine cathode materials. Sample E75 shows a slight increase in the unit cell parameter of a_{hex} , but samples E80 and E85 show a

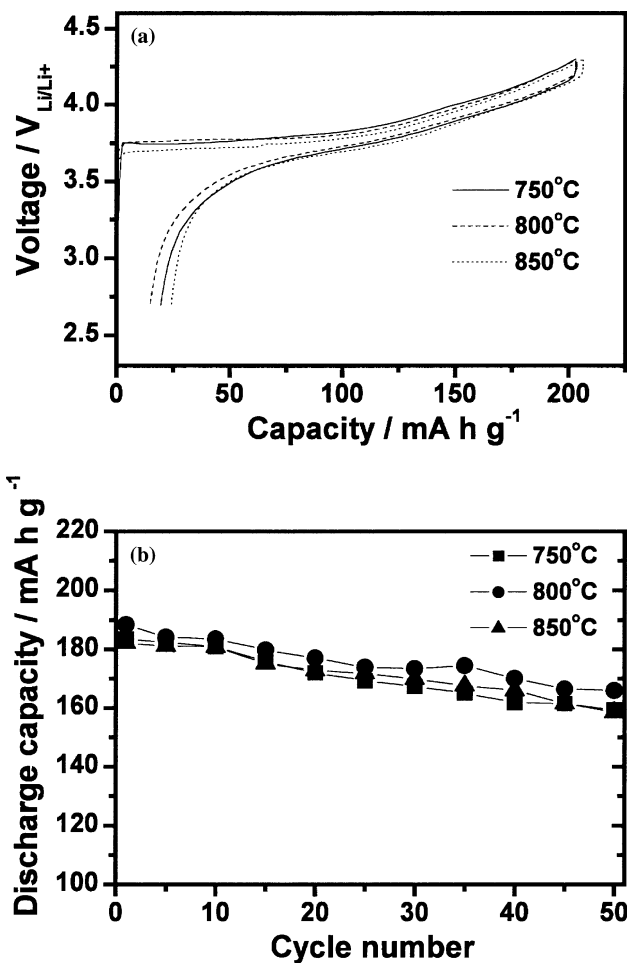


Fig. 5. Initial charge and discharge curves (a) and discharge capacities (b) as a function of the number of cycles of the synthesized cathode materials in the voltage range 2.7 $\text{V}_{\text{Li}^+/\text{Li}}$ to 4.3 $\text{V}_{\text{Li}^+/\text{Li}}$.

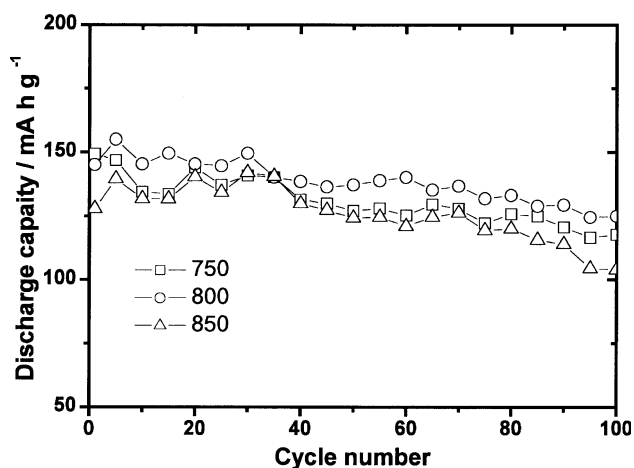


Fig. 6. Cycle stability for the synthesized compounds at the 1 C rate (200 mA g^{-1}) of the charge-discharge experiment between 2.7 $\text{V}_{\text{Li}^+/\text{Li}}$ and 4.2 $\text{V}_{\text{Li}^+/\text{Li}}$.

slight decrease after the cycling test. According to Croguennec et al., the increase in the a_{hex} parameter after the first cycle indicates that the cation migration

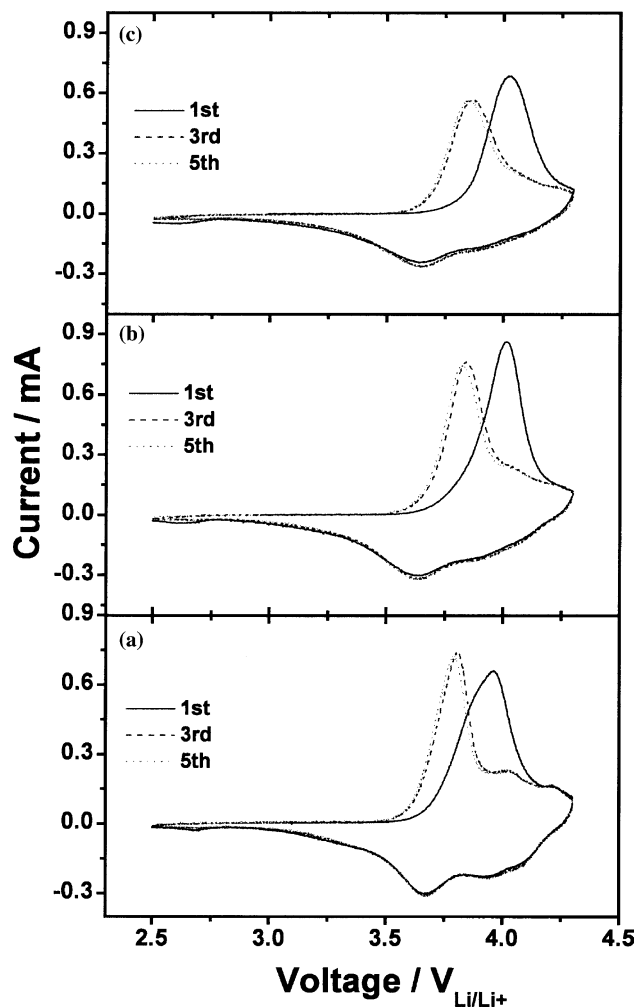


Fig. 7. Cyclic voltammogram of $\text{LiNi}_{0.8}\text{Co}_{0.2}\text{O}_2$ powders calcined at (a) 750 °C, (b) 800 °C and (c) 850 °C in the voltage range 2.5 $V_{\text{Li}^+/\text{Li}}$ to 4.3 $V_{\text{Li}^+/\text{Li}}$.

from the slab (NiO_6) to the interslab (LiO_6) space induces cation mixing [23]. After a long-range cycling experiment, Poullierie et al. reported a similar phenomenon [24]. Consequently, this result suggests that the structural degradation of E75 is more serious than that of E80 or E85 during cycling. The smallest change in the volume of a unit cell was observed with the E80 sample over 100 cycles. Lithium extraction from the cathode material leads to shrinkage of the unit cell volume which is then reversibly restored during insertion of lithium to the cathode. As a result, the decrease in the unit cell volume after the cycle test can be considered as a decrease in the reversible capacity. We therefore believe that the better cycle life of E80

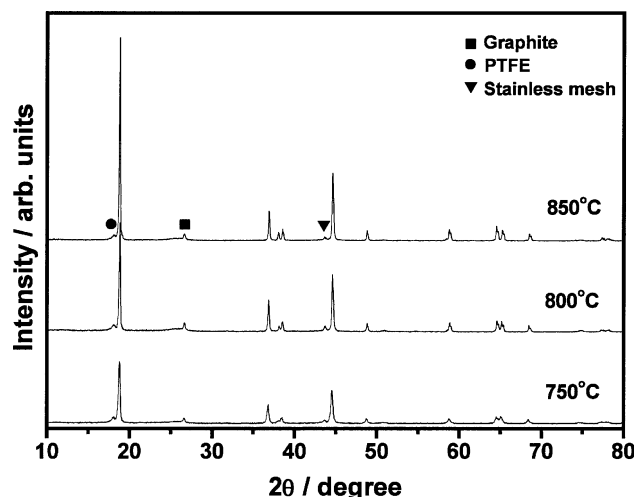


Fig. 8. X-ray diffraction patterns of $\text{LiNi}_{0.8}\text{Co}_{0.2}\text{O}_2$ powder after 100 cycles.

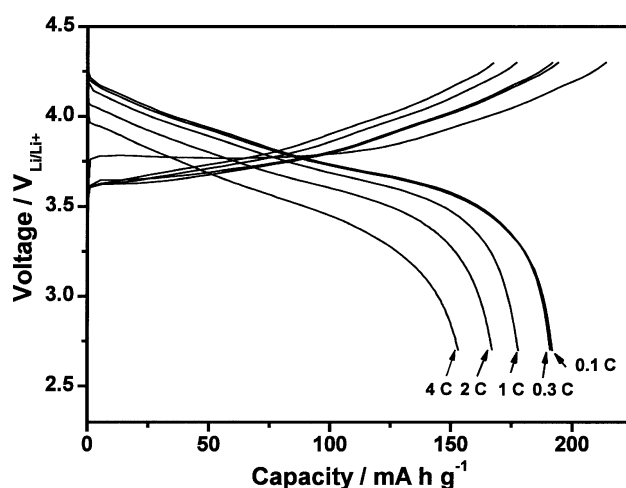


Fig. 9. Rate capability test for the sample prepared at 800 °C between 2.7 $V_{\text{Li}^+/\text{Li}}$ and 4.3 $V_{\text{Li}^+/\text{Li}}$.

than others is related to the better structural stabilization of the material during the charge-discharge process and lower degree of cation mixing, as shown by Rietveld analysis.

To investigate the rate capability of the $\text{LiNi}_{0.8}\text{Co}_{0.2}\text{O}_2$ prepared at 800 °C, we applied various C rates of 0.1 C, 0.3 C, 1 C, 2 C and 4 C to the electrode in the voltage range 2.7 $V_{\text{Li}^+/\text{Li}}$ to 4.3 $V_{\text{Li}^+/\text{Li}}$. The C rates were calculated using 200 mA h g^{-1} as a theoretical capacity. Figure 9 shows the results. The discharge capacity of the cathode was 191.8 mA h g^{-1} at the initial cycle; it then gradually decreased as the C rate increased. Even when

Table 2. Comparison of the structural parameters between pristine and cycled cathode materials prepared at different calcination conditions

Calcination temp./°C	Pristine cathode			Cycled cathode			$\Delta V/\text{Å}^3$
	$a/\text{Å}$	$c/\text{Å}$	Vol./ Å^3	$a/\text{Å}$	$c/\text{Å}$	Vol./ Å^3	
750	2.8640(2)	14.162(1)	100.62	2.8644(7)	14.195(4)	100.87	0.25
800	2.8648(1)	14.164(1)	100.67	2.8605(9)	14.180(4)	100.48	-0.19
850	2.8660(1)	14.164(1)	100.76	2.8580(9)	14.200(5)	100.45	-0.31

4 C (800 mA g⁻¹) was applied to the electrode, the electrode could deliver a highly retained discharge capacity of 153.1 mA h g⁻¹, which corresponds to 80 percent of the initial discharge capacity. As shown above, the cathode material shows a good rate capability, which may be due to the nature of the LiNi_{0.8}Co_{0.2}O₂ cathode that was synthesized by the emulsion drying method; for example, small particles and good structural integrity.

4. Conclusion

We have successfully synthesized LiNi_{0.8}Co_{0.2}O₂ powders by using the emulsion drying method. Structural analysis with the XRD Rietveld method shows that 800 °C is an appropriate calcination temperature for obtaining well-ordered and lower cation mixed LiNi_{0.8}Co_{0.2}O₂ powder. Our electrochemical experiments show that the powder prepared at 800 °C delivers the highest discharge capacity of 188.4 mA h g⁻¹, and the same powder has the highest capacity retention ratio of 88.1% at 0.2 C and 86.8% at 1 C rate. Moreover, the rate capability test reveals that this cathode can deliver a high discharge capacity of 153 mA h g⁻¹ at a rate of 4 C (800 mA g⁻¹). We conclude, therefore, that the emulsion drying method is an attractive method for synthesizing layered LiNi_{0.8}Co_{0.2}O₂ cathode material, and that 800 °C is the optimal calcination temperature.

Acknowledgement

This work was supported by a grant from the Basic Research Program of the Korea Science and Engineering Foundation.

References

1. T. Ohzuku, A. Ueda and M. Nagayama, *J. Electrochem. Soc.* **140** (1993) 1862.
2. A. Rougier, J. Saadoune, P. Gravereau, P. Willmann C. Delmas, *Solid State Ionics* **90** (1996) 83.
3. J.N. Reimers, E. Rossen, C.D. Jones and J.R. Dahn, *Solid State Ionics* **61** (1993) 335.
4. Q. Zhong and U. von Sacken, *J. Power Sources* **54** (1995) 221.
5. A. Hirano, R. Kanno, Y. Kawamoto, Y. Nitta, K. Okamura T. Kamiyama and F. Izumi, *J. Solid State Chem.* **134** (1997) 1.
6. J. Kim and K. Amine, *J. Power Sources* **104** (2002) 33.
7. G. Prado, A. Rougier, L. Fournes and C. Delmas, *J. Electrochem. Soc.* **147** (2000) 2880.
8. C. Pouillierie, L. Croguennec, Ph. Biensan, P. Willmann C. Delmas, *J. Electrochem. Soc.* **147** (2000) 2061.
9. A. Rougier, P. Gravereau and C. Delmas, *J. Electrochem. Soc.* **143** (1996) 1168.
10. I. Saadoune and C. Delmas, *J. Mater. Chem.* **6**(2) (1996) 193.
11. I. Saadoune and C. Delmas, *J. Solid State Chem.* **136** (1998) 8.
12. D. Caurant, N. Baffler, B. Garcia and J.P. Pereira-Ramos, *Solid State Ionics* **91** (1996) 45.
13. Y.M. Choi, S.I. Pyun, S.I. Moon and Y.E. Hyung, *J. Power Sources* **72** (1998) 83.
14. W. Li, J.C. Currie and J. Wolstenholme, *J. Power Sources* **68** (1997) 565.
15. S.T. Myung, S. Komaba, N. Kumagai, H. Yashiro, H.T. Chung and T.H. Cho, *Electrochimica Acta* **47** (2002) 2543.
16. S.T. Myung, N. Kumagai, S. Komaba and H.T. Chung, *Solid State Ionics* **139** (2001) 47.
17. S.T. Myung and H.T. Chung, *J. Power Sources* **84** (1999) 32.
18. T. Roisnel and J. Rodriguez-Carjaval, Fullprof Manual, Institut Laue-Langevin, Grnoble (2000).
19. G.X. Wang, J. Horvat, D.H. Bradhurst, H.K. Liu and S.X. Dou, *J. Power Sources* **85** (2000) 279.
20. J.R. Dahn, U. von sacken and A.V. Chadwick, *Solid State Ionics* **44** (1990) 87.
21. J. Cho and B. Park, *J. Power Sources* **92** (2001) 35.
22. K. Dokko, M. Nishizawa, S. Horikoshi, T. Itoh, M. Mohamed and I. Uchida, *Electrochem. Solid State Lett.* **3** (1999) 3.
23. L. Croguennec, C. Pouillierie and C. Delmas, *J. Electrochem. Soc.* **147** (2000) 1314.
24. C. Pouillierie, L. Croguennec and C. Delmas, *Solid State Ionics* **132** (2000) 15.